International Journal of Medical Microbiology 306 (2016) 187–195

Contents lists available at ScienceDirect

International Journal of Medical Microbiology

journal homepage: www.elsevier.com/locate/ijmm

The absence of microbiota delays the inflammatory response to *Cryptococcus gattii*

Marliete Carvalho Costa[a,1], Julliana Ribeiro Alves Santos[a,1], Maira Juliana Andrade Ribeiro[a,1], Gustavo José Cota de Freitas[a], Rafael Wesley Bastos[a], Gabriella Freitas Ferreira[a,d], Aline Silva Miranda[b], Raquel Duque Nascimento Arifa[a], Patrícia Campi Santos[a], Flaviano dos Santos Martins[a], Tatiane Alves Paixão[c], Antonio Lúcio Teixeira[b], Danielle G. Souza[a], Daniel Assis Santos[a,*]

[a] Departamento de Microbiologia, Instituto de Ciências Biológicas, Universidade Federal de Minas Gerais, Belo Horizonte, MG 31270-901, Brazil
[b] Laboratório Interdisciplinar de Investigação Médica, Faculdade de Medicina, Universidade Federal de Minas Gerais, Belo Horizonte, MG 30130-100 Brazil
[c] Departamento de Patologia Geral, Instituto de Ciências Biológicas, Universidade Federal de Minas Gerais, Belo Horizonte, MG 31270-901, Brazil
[d] Departamento de Farmácia, Universidade Federal de Juiz de Fora—Campus Governador Valadares, Governador Valadares, MG 35020-220, Brazil

ARTICLE INFO

Article history:
Received 4 November 2015
Received in revised form 14 March 2016
Accepted 28 March 2016

Keywords:
Cryptococcus gattii
Cryptococcosis
Germ-free mice
Microbiota

ABSTRACT

The inflammatory response plays a crucial role in infectious diseases, and the intestinal microbiota is linked to maturation of the immune system. However, the association between microbiota and the response against fungal infections has not been elucidated. Our aim was to evaluate the influence of microbiota on *Cryptococcus gattii* infection. Germ-free (GF), conventional (CV), conventionalized (CVN—mice that received feces from conventional animals), and LPS-stimulated mice were infected with *C. gattii*. GF mice were more susceptible to infection, showing lower survival, higher fungal burden in the lungs and brain, increased behavioral changes, reduced levels of IFN-γ, IL-1β and IL-17, and lower NFκBp65 phosphorylation compared to CV mice. Low expression of inflammatory cytokines was associated with smaller yeast cells and polysaccharide capsules (the main virulence factor of *C. gattii*) in the lungs, and less tissue damage. Furthermore, macrophages from GF mice showed reduced ability to engulf, produce ROS, and kill *C. gattii.* Restoration of microbiota (CVN mice) or LPS administration made GF mice more responsive to infection, which was associated with increased survival and higher levels of inflammatory mediators. This study is the first to demonstrate the influence of microbiota in the host response against *C. gattii.*

1. Introduction

Cryptococcus gattii causes cryptococcosis, affecting the lungs and central nervous system (CNS) of immunocompetent individuals, and cryptococcal meningoencephalitis is the most severe clinical manifestation (Perfect et al., 2010; Franco-Paredes et al., 2015). Severe *C. gattii* infection is due to defective induction of the host immune response, resulting in low levels of proinflammatory cytokines (Brouwer et al., 2007). During infection, important changes occur in the capsular polysaccharides and cell morphology, affecting pathogenicity (Okagaki et al., 2010a,b).

Axenic animals, created in sterile conditions without microbiota contact and colonization (Germfree—GF), have been used as a model to study the effect of the absence of microorganism on the host physiology and anatomy (Yi and Li, 2012). The gut microbiota regulates the development and maturation of the immune system (Kamada et al., 2013). Compared to conventionally raised mice, GF mice show reduced Peyer's patches (Sommer and Bäckhed, 2013), mesenteric lymph nodes (Round and Mazmanian, 2009), cytokine production, serum immunoglobulin levels (Kamada et al., 2013), and hematopoiesis (Khosravi et al., 2014). These features make GF animals more susceptible to infection by bacteria (Khosravi et al., 2014), e.g., *Listeria monocytogenes* (Inagaki et al., 1996; Mittrücker et al., 2014), *Salmonella enterica* Typhimurium (Nardi et al., 1989), and *Klebsiella pneumoniae* (Fagundes et al., 2012). The absence

* Corresponding author at: Departamento de Microbiologia, Instituto de Ciências Biológicas, Universidade Federal de Minas Gerais, Av. Antonio Carlos, 6627, Pampulha, Belo Horizonte, Minas Gerais 31270-901, Brazil.
E-mail address: das@ufmg.br (D.A. Santos).
[1] These authors contributed equally to this study.

http://dx.doi.org/10.1016/j.ijmm.2016.03.010
1438-4221/

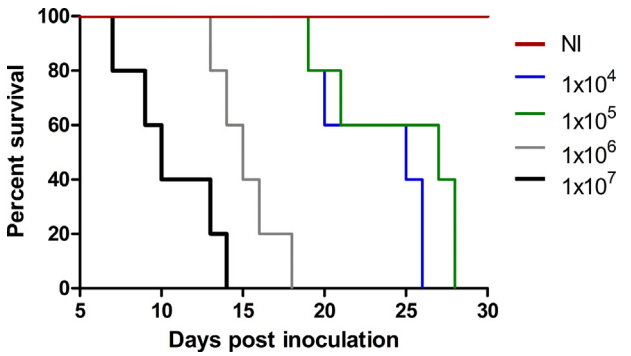

Fig. 1. *Cryptococcus gattii* induces lethality in germfree (GF) mice in an inoculum-dependent manner.
GF mice (n = 6) were inoculated by the intratracheal route with 1×10^4, 1×10^5, 1×10^6, or 1×10^7 *C. gattii* cells. Mice in the uninfected group (NI) were administered PBS. The results shown are percent survival postinfection.

of microorganisms can have either a negative (Ichinohe et al., 2011) or positive (Kuss et al., 2011) effect on viral infection (Wilks et al., 2013). Although these studies demonstrated the role of host microbiota on viral and bacterial infections, the effects on fungal infections are not yet known.

The aim of this study was to investigate the influence of gut microbiota on murine cryptococcosis caused by *C. gattii*. Our data demonstrate that the absence of microbiota leads to a delayed inflammatory response and morphological alterations in the yeasts during cryptococcosis.

2. Material and methods

2.1. Animals and ethics

GF *Swiss*/NIH mice (6–8-weeks old) from the GF nucleus (Taconic, Germantown, NY, USA) and *Swiss* conventional (CV) mice were used in this study. GF mice were maintained in flexible plastic isolators (Standard Safety Equipment) using classical gnotobiology techniques. As a microbiological control, fecal samples were plated on thioglycollate broth and brain heart infusion (BHI) broth and incubating at 37 °C (Pedroso et al., 2015). Groups of GF mice were subjected to conventionalization (CVN mice; i.e., fecal samples removed from the large intestine of CV mice were homogenized in saline [10%] and administered by oral gavage to GF mice, which were colonized for 21 days prior to intratracheal [i.t.] inoculation of *C. gattii*) (Souza et al., 2004). CVN mice were i.t. infected with *C. gattii* in the next day after the conventionalization was completed. Other groups received LPS (*Escherichia coli* 0111: B4, 4 mg/kg; Sigma-Aldrich) i.p. 48 h prior to *C. gattii* inoculation. The animal protocol was approved by the Comitê de Ética no Uso de Animais (CEUA) of Universidade Federal de Minas Gerais (Protocol 287/2012). Mice were sacrificed under anesthesia (i.p. ketamine [60 mg/kg] and xylazine [10 mg/kg]) by cervical dislocation.

2.2. Infection of mice with C. gattii

The L27/01 strain of *C. gattii* was cultured on Sabouraud dextrose agar (SDA) for 48 h at 35 °C and colonies were suspended in PBS to generate inoculum at 1×10^4, 1×10^5, 1×10^6, or 1×10^7 CFU/animal. Mice (n = 6/group) were anesthetized by i.p. injection of ketamine hydrochloride (80 mg/kg) and xylazine (15 mg/kg) in sterile saline and inoculated (i.t.) with 30 μL of cryptococcal cells and were monitored daily to determine the inoculums to use in subsequent experiments (Santos et al., 2014).

2.3. Fungal burden, myeloperoxidase (MPO) and β-N-acetylglucosaminidase (NAG) activities, cytokine and chemokine levels, NFκBp65 phosphorylation, and histopathology

GF, CV, CVN, and LPS-stimulated mice were inoculated (i.t.) with 1×10^7 CFU/animal (standardized inoculum) or PBS only (control). Lungs and brain were obtained at 1 or 10 days post inoculation, homogenized in PBS and plated onto SDA for measurement of fungal burden (Maxeiner et al., 2007).

The MPO assay and cytokine analysis was performed according to Elian et al. (2015) and NAG assay according to Aires et al. (2013), both with modifications. MPO and NAG assay were used as an indirect measurement of neutrophil and macrophages accumulation in lungs, respectively. Briefly, 100 mg of the lungs were used for cytokines analysis and MPO/NAG assays. The tissue was homogenized with 1 mL of PBS (pH 7.0) containing anti-proteases (0.1 mM PMSF, 0.1 mM benzethonium chloride, 10 mM EDTA and 20 Kallikrein inhibitor units of aprotinin A, all purchased from Sigma-Aldrich and 0.05% tween 20). The samples were centrifuged for 10 min at 3000*g*, at 4 °C and the supernatant was frozen at −20 °C and utilized for cytokines analysis. The levels of cytokines TNF-α, IFN-γ, IL-1β, IL-10 and IL-17 was determined by ELISA with commercially available antibodies according to the procedures supplied by the manufacturer (R&D Systems, Minneapolis, MN, USA).

The pellet obtained as described above was resuspended in 1.9 mL of buffer, pH 4.7 (0.1 M NaCl, 0.02 M $NaH_2PO_4 \cdot 1H_20$, 0.015 M Na_2-EDTA) and centrifuged again (12,000 *g* for 10 min). The supernatant was discarded and to the precipitate was added 0.9 mL of 0.2% NaCl solution followed by addition of an equal volume of solution containing 1.6% NaCl and 5% glucose. After homogenization, the content was equally divided into two new tubes, one for MPO assay and another for NAG assay. The tubes were centrifuged (12,000*g*, at 4 °C, for 10 min), the supernatant discarded and the pellet resuspended in 0,6 mL of 0.05 M $NaPO_4$buffer (pH 5.4) containing 0.05% hexadecytrimethyl-amonium bromide (HTAB) (Sigma-Aldrich) for MPO assay and in 0.6 mL 0.9% saline solution containing 0.1% (v/v) Triton X-100 for NAG assay. After frozen three times in liquid nitrogen, the content was centrifuged at 4 °C at 12,000*g* for 10 min. The supernatant was collected in a new tube and kept in −80 °C.

For MPO assay, 25 μL of the supernatant was added to microplates of 96 wells, in triplicate, following addition of same volume of 3,3′,5,5′-Tetramethylbenzidine (TMB) (Sigma-Aldrich) and incubation at 37 °C for 5 min. After that, 100 μL of 0.002% (v/v) H_2O_2 was added and the samples were again incubated at 37 °C for 5 min. After the incubation period, the reaction was stopped by adding 100 μL1 M H_2SO_4. The absorbance reading was taken at 450 nm. The result was expressed in MPO/100 mg of tissue.

For NAG assay, the supernatant was diluted in citrate-phosphate buffer, pH 4.5 (0.1 M citric acid and 0.1 M Na_2HPO_4), in proportion of 1:3, and100 μL of each diluted sample was added in microplate of 96 wells, in triplicate. Then, 100 μL 2,24mMp-nitrophenyl-*N*-acetyl-β-D-glicosaminide (Sigma-Aldrich) substrate diluted in a citrate-phosphate buffer was added in each well and the microplate was incubated at 37 °C for 5 min. After reaction, 100 μL of 0.2 M glycine buffer, pH 10.6 (0.8 M glycine, 0.8 M NaCl and 0.8 M NaOH) were added to stop the reaction. The absorbance was read at 400 nm. The result was expressed in NAG/100 mg of tissue.

NFκBp65 phosphorylation levels in the lungs of GF and CV mice was determined by western blotting (Lv et al., 2014). Briefly, samples containing 30 μg of protein were resolved on an SDS-PAGE gel and transferred to a PVDF membrane. The membrane was incubated with specific primary antibodies (1:2000; Sigma, St. Louis, MO, USA) and then with a secondary anti-mouse HRP-conjugated antibody (1:5000; Amersham), and the signal was quantified using

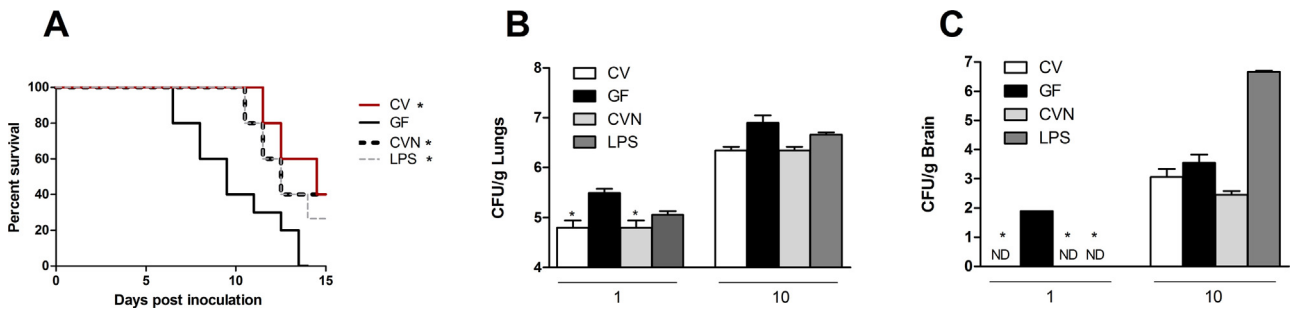

Fig. 2. Lack of microbiota turns GF mice more susceptible to infection, showing lower survival and higher fungal burden in the lungs and brain.
n = 6 animals per group were inoculated by the intratracheal route with 1×10^7 *C. gattii* cells. Results shown are percent survival postinfection (A). At 1 or 10 days post inoculation, mice were sacrificed. The CFU of yeasts per g of lung (B) or brain (C) were determined. CV: conventional mice; GF: germ-free mice; CVN: conventionalized mice; LPS: LPS-stimulated mice; ND: not-detected. *p: were significantly different from GF mice ($p < 0.05$).

a chemiluminescence system (Santa Cruz Biotechnology, Santa Cruz, CA, USA).

In addition, organs were stained with hematoxylin-eosin.

2.4. Phagocytosis assay, intracellular proliferation rate (IPR) determination, and measurement of reactive oxygen species (ROS) production by macrophages

Murine peritoneal macrophages were used to assess phagocytic index, ROS production, and the IPR of *C. gattii* (Ma et al., 2009). GF, CV, and CVN mice were stimulated with i.p. injection with 1.5 mL of 3% thioglycolate (300 mg thioglycolate, 42 mg $NaHCO_3$, 10 mL of PBS). Four days later, mice were sacrificed under anesthesia by cervical dislocation and the peritoneal exudate cells were harvested by two cycles of injection of 5 mL of cold RPMI 1640 (GIBCO). Collected cells were washed by centrifugation at 290*g* for 5 min, resuspended in RPMI 1640 supplemented with 100 U/mL penicilin, 100 mg/mL estreptomicin (GIBCO), and 10% fetal bovine serum (Sigma). Briefly, 500 μL of murine macrophages (1×10^5 cells/well) in RPMI were plated into 24-well plates and incubated overnight at 37 °C under 5% CO_2. Then, the culture supernatant was removed and adherent macrophages were infected with 500 μL of suspension containing 3×10^4 cells/well viable yeasts (proportion 3:1 of macrophages:cryptococcus), and after 0 and 24 h post infection, phagocytic index and IPR were analized.

The phagocytic index was calculated as the percentage of cells with internalized *C. gattii* 24 h post infection (Santos et al., 2014). In addition, the intracellular proliferation rate (IPR) assay was performed as described previously (Ma et al., 2009) with modifications. Non-internalized yeast cells in the supernatant were taken from the wells and washed with 200 μL PBS. Macrophages were lysed at 24 h with 200 μL of cold sterile distilled water and incubated for 30 min at 37 °C, then 200 μL was collected and mixed with Trypan Blue in a 1:1 ratio, and the viable yeast cells were counted. Intracellular proliferation rate was calculated as the quotient of the intracellular yeast cell numbers at 24 h and 0 h.

Endogenous amounts of ROS were measured by fluorometric assay with specific probes. 0.2×10^5 macrophages/well in RPMI-1640 without phenol red (Sigma-Aldrich), supplemented with 100 U/mL penicilin, 100 mg/mL estreptomicin (GIBCO), and 10% fetal bovine serum (Sigma), were plated into 96-well plates and incubated overnight at 37 °C under 5% CO_2. Macrophages were then infected with yeast 0.6×10^4 cels/well (proportion 3:1 of macrophages:cryptococcus), and incubated for 24 h at 37 °C under 5% CO_2. To quantify ROS production, 10 mM 2′,7′-dichlorofluorescein diacetate (Invitrogen, Life Technologies, Carlsbad, CA, USA) was added. For both the protocols, the probe was add 30 min prior the mensuration with a fluorometer (Synergy 2 SL Luminescence Microplate Reader; Biotek) using excitation and emission wavelengths of 500 nm (Ferreira et al., 2013).

2.5. Behavioral analysis

The SmithKline/Harwell/Imperial College/Royal Hospital/Phenotype Assessment (SHIRPA) protocol for behavioral and functional assessment of neurological diseases in animal models (Rogers et al., 1997; Rogers et al., 2001), was used in this study. This provides reliable information on cerebral dysfunction and general status of mice. GF, CV, CVN, and LPS mice were inoculated with *C. gattii* or PBS (control). At 10 days post infection, the SHIRPA protocol was applied to all groups of mice. The tasks assessed by SHIRPA were grouped into five functional categories: neuropsychiatric state, motor behavior, autonomic function, muscle tone and strength, and reflex and sensory function (available in the Supplementary Table S1) (Lackner et al., 2006; Pedroso et al., 2013; Santos et al., 2014). Changes in each functional category were expressed as scores to assess behavioral performance.

2.6. Cell diameter, capsule size, and zeta potential measurements of C. gattii

Colonies recovered from the lungs of GF, CV, and CVN mice at 1 or 10 d.p.i. were used for morphometric analyses and zeta potential measurements as previously described (Ferreira et al., 2015).

2.7. Statistical analysis

All statistical analyses were performed using GraphPad Prism (version 5.0;GraphPad Software, San Diego CA, USA). $P < 0.05$ was considered statistically significant and all groups (CV, CVN, LPS) were analyzed in comparison to GF mice. Survival was plotted as a Kaplan-Meier curve and analyzed using the log rank test. Fungal burden, phagocytosis, IPR, MPO, NAG, and cytokine and chemokine levels were analyzed by ANOVA and the nonparametric Friedman test. SHIRPA data were analyzed with the Wilcoxon Rank-Sum Test (Pedroso et al., 2010).

3. Results

3.1. C. gattii induces lethality in GF mice in an inoculum-dependent manner

GF mice inoculated with 1×10^6 or 1×10^7 CFU showed signs of cryptococcosis earlier than mice administered with 1×10^4 and 1×10^5 CFU. Animals infected with all inoculum succumbed to infection dependently of fungi load of infection. Mice injected with

1×10^7 yeasts succumbed after 14 days post infection (d.p.i.) (Fig. 1) and this inoculum was chosen for all subsequent experiments.

3.2. Lack of microbiota turns GF mice more susceptible to infection

GF mice succumbed to infection earlier than CV animals (Fig. 2A). Microbiota restoration and systemic administration of LPS improved the survival of GF mice (Fig. 2A). A higher fungal burden in the lungs of GF mice was found at 1 d.p.i. (Fig. 2B), and *C. gattii* reached the CNS of GF mice within 1 day after infection (Fig. 2C). However, at 10 d.p.i., there was no statistical difference in the lung or brain of GF and CV mice (Fig. 2B and C). Conventionalization reduced the fungal burden in the lungs (at 10 d.p.i.; Fig. 2B) and brain (at 1 d.p.i.; Fig. 2C) of CVN mice. Although the fungal burden in the lungs (Fig. 2B) and brain (Fig. 2C) of LPS-administered mice was similar to that in GF mice, LPS prevented *C. gattii* dissemination to the brain at the beginning of the infection (Fig. 2C).

3.3. Germ-free mice showed a delayed inflammatory response

The MPO activity in the lungs (Fig. 3A), production of IFN-γ (Fig. 3B), IL-17 (Fig. 3C), IL-1β (Fig. 3D) and TNF-α (data not show) in the lungs and NF-κBp65 (Fig. 3E–F) phosphorylation were significantly reduced ($p < 0.05$) in GF mice at 1 d.p.i. Only IL-10 (data not show) levels in the lungs were similar in GF and CV mice ($p > 0.05$) at 1 d.p.i. At 10 d.p.i., the MPO activity and the levels of IL-1β (Fig. 3A and D) were similar between all the groups of mice ($p > 0.05$). However the production of IFN-γ (Fig. 3B) was lower for CVN and LPS mice and the levels of IL-17 (Fig. 3C) and IL-10 (data not shown) were higher for GF mice in comparison with all the other groups.

There were no differences in the activity of MPO (Fig. 3A) into the lung when the microbiota was restored. CVN mice showed higher expression of TNF-α (data not show), IFN-γ (Fig. 3B), IL-17 (Fig. 3C) and IL-1β (Fig. 3D) in the lungs at 1 d.p.i., with decreased levels of these cytokines at 10 d.p.i. Lower levels of IL-17 (Fig. 3C) and IL-10 (data not show) were also detected at 10 d.p.i. in CVN mice. Administration of LPS did not alter the MPO activity (Fig. 3A) in lungs. However LPS increased the levels of IFN-γ, IL-17 and IL-1β (Fig. 3B–D) in the lungs ($p < 0.05$) after 1 d.p.i.; but IFN-γ and IL-17 levels (Fig. 3B–C) were significantly reduced at 10 d.p.i.

Similar NAG activity, an indirect measure of macrophage recruitment, was verified for GF, CV and CVN mice ($p > 0.05$, data not shown). Otherwise, administration of LPS increased the NAG activity in the lungs at 10 d.p.i. in comparison to GF mice (NAG activity for LPS = 0.22 ± 0.056 *vs.* NAG activity for GF = 0.15 ± 0.06 NAG/100 mg of lung).

3.4. Macrophages recovered from GF mice showed reduced ability to engulf, produce ROS, and kill C. gattii

In the phagocytosis assay, fewer fungi were engulfed by macrophages from GF mice than by macrophages from CV mice ($p < 0.05$; Fig. 4A). Macrophages from CVN mice showed the same ability to engulf *C. gattii* that GF (Fig. 4A). However, *C. gattii* proliferated at a greater rate inside GF macrophages (Fig. 4B) and lower levels of ROS were produced in this group of mice ($p < 0.05$; Fig. 4C).

3.5. Morphological alterations in C. gattii cells recovered from GF, CV and CVN mice

Fungi recovered from the lungs of GF mice (Fig. 5A) were smaller than those recovered from CVN (Fig. 5B) and CV (Fig. 5C). Indeed, these data are represented in Fig. 5D (whole cell diameter) and 5E (capsule size). The cellular charges, expressed as the zeta potential, was more negative for colonies recovered from CV mice at 10 d.p.i. in comparison to GF and CVN mice (Fig. 5F)

3.6. Delayed inflammation in GF mice was associated with reduced tissue damage

Fungal translocation to the CNS of infected GF mice occurred faster compared to that in CV, CVN, and LPS-stimulated mice (Fig. 6A and B). In the lungs, GF mice showed a higher number of yeast in the alveolar lumen and mild inflammation (Fig. 6E). CV, (Fig. 6F), CVN (Fig. 6G) and LPS (Fig. 6H) mice presented moderate to intense inflammation and numerous yeasts.

3.7. GF mice showed prominent behavioral alterations associated with cryptococcosis

The behavioral assessment scores of GF, CV, CVN, and LPS-stimulated mice compared to those of uninfected mice (NI) are presented in Table 1. Although all of the mice in the infected groups showed changes in muscle tone and strength, GF mice were unique, presenting prominent alterations ($p < 0.05$) in motor behavior and reflex and sensory function.

4. Discussion

GF animals are important tools for evaluating the role of microbiota on different conditions (Fagundes et al., 2012; Wilks et al., 2013), but little is known about it in fungal diseases. Our data showed that microbiota is important for the host response against *C. gattii*; GF mice succumbed early, and showed a delayed inflammatory response, which enabled translocation of *C. gattii* to the brain within 1 d.p.i. The higher fungal burden in lungs and brain of GF mice infected with *C. gattii* indicates that the response on these mice is not sufficient to control the fungal growth and translocation. This result was corroborated by the higher intracellular proliferation rate within the macrophages of GF mice (due to low ROS production), since it has been well established that translocation from the lungs to the CNS depends on fungal survival inside phagocytes (Charlier et al., 2009).

The delayed inflammatory response of GF mice was also evidenced by the lower levels of proinflammatory mediators and cell recruitment to the lungs. These data were confirmed by the lower NFκBp65 phosphorylation levels in the lungs of GF mice. In this context, TLR activation by the bacterial products of the microbiome may lead to homeostasic activation of NFκB and upregulation of the proinflammatory cytokines that facilitate host defense against the pathogen (Lavelle et al., 2010). Another study showed that a lack of microbiota primarily impairs the early recruitment and activation of granulocytes (Mittrücker et al., 2014), probably due a primary defect in hematopoiesis (Khosravi et al., 2014). Low production of proinflammatory mediators was reported in previous studies with GF mice (Fox et al., 2012). Interestingly, GF mice showed increased production of proinflammatory cytokines after 10 d.p.i., demonstrating a later immune response. This has not been previously described since other studies followed GF mice until a maximum of 72 h after infection or other stimuli (Fagundes et al., 2012). It is likely that the immune system was stimulated by the pathogen during the first 10 days of infection.

Moreover, yeasts have developed complex strategies to ensure their adaptation under different conditions. Within the host, the cryptococcal cells alter its morphology and physiology to survive under the immune system pressure. By modifying the capsule and the whole cell diameter, the pathogen may inhibit phagocytosis, which is crucial for the host response in the early phase of the infection (Zaragoza et al., 2010). In our study, GF mice showed lower levels of proinflammatory mediators, leading to reduced

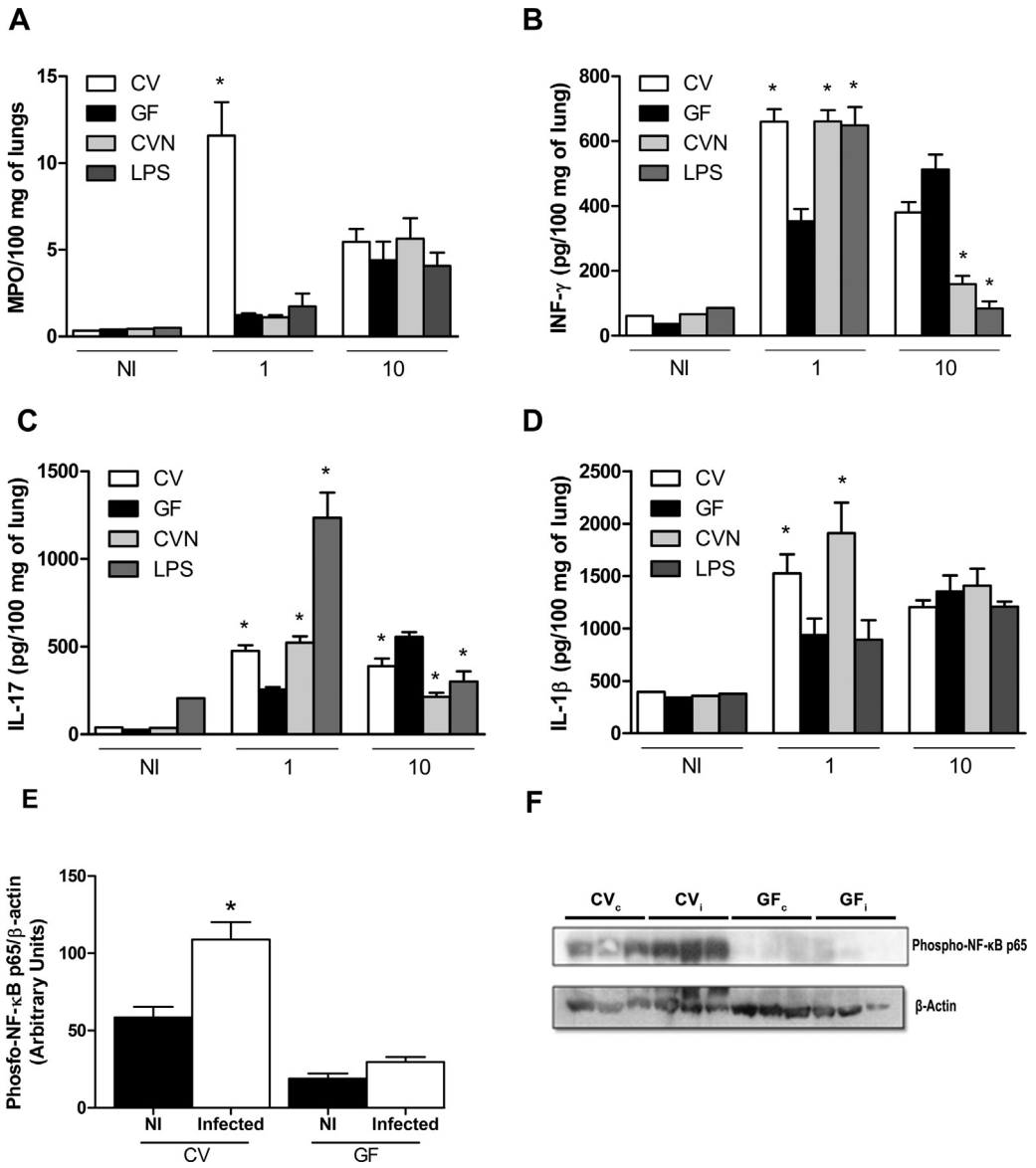

Fig. 3. Germ free mice showed a delayed inflammatory response.
n = 6 animals per group were inoculated by the intratracheal route with 1×10^7 *C. gattii* cells or PBS (NI). After 1 or 10 d.p.i., mice were sacrificed. MPO activity in the lungs was used as an index of neutrophil influx in the tissue (A). Levels of IFN-γ (B), IL-17 (C) and IL-1β (D) are expressed as pg per 100 mg of lung. Quantitative densitometry (E) of the western blot (F) of the expression of phosphorylated NFκBp65 in CV and GF mice (CV_c: non-infected conventional mice, GF_c: non-infected germ-free mice, CV_i: infected conventional mice, GF_i: infected germ-free mice). CV: conventional mice; GF: germ-free mice; CVN: conventionalized mice; LPS: LPS-stimulated mice. *p: were significantly different from GF mice ($p < 0.05$).

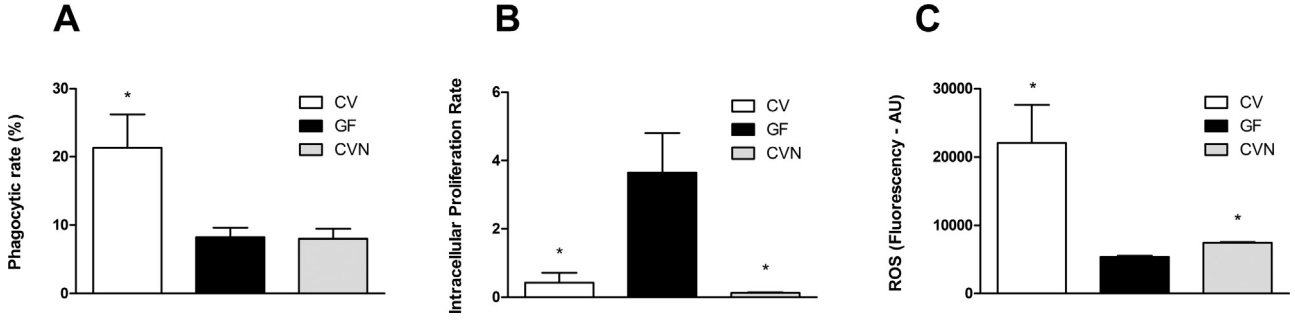

Fig. 4. Macrophages recovered from GF mice showed reduced ability to engulf, produce ROS, and kill *C. gattii*.
Murine peritoneal macrophages from GF, CV, and CVN mice were infected with *C. gattii*. The phagocytic index was calculated as the percentage of macrophages (A) with internalized *C. gattii*. Intracellular Proliferation Rate (B).The amount of reactive oxygen species (ROS) is expressed in arbitrary units of fluorescence (AU) (C). CV: conventional mice; GF: germ-free mice; CVN: conventionalized mice. *p: were significantly different from GF mice ($p < 0.05$).

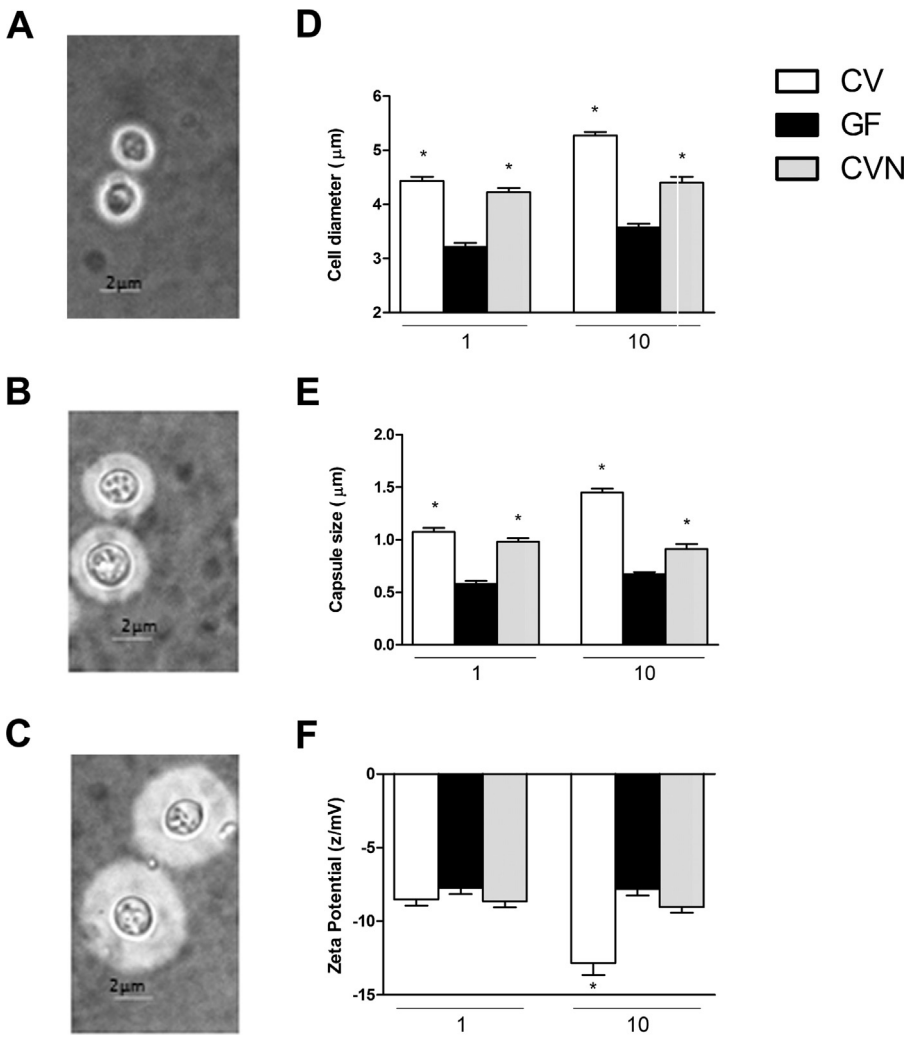

Fig. 5. Morphological alterations in *C. gattii* cells recovered from GF, CV and CVN mice.
CV, GF, and CVN mice were inoculated by the intratracheal route with 1×10^7 *C. gattii* cells. At 1 and 10 d.p.i., the mice were sacrificed, and yeasts were recovered from the lungs. Microscopic visualization of India ink-stained cells recovered from GF at 10 d.p.i. (A), CVN (B), and CV mice (C). Cell diameter (D) and capsule (E) size were determined by India ink counter staining. The zeta potential of yeast cells was calculated (F). CV: conventional mice; GF: germ-free mice; CVN: conventionalized mice; *p: were significantly different from GF mice ($p < 0.05$).

Table 1
GF mice showed prominent behavioral alterations associated with cryptococcosis. Scores from the assessment of behavioral performance in GF, CV, CVN, and LPS-infected mice compared to the uninfected group (NI) at 10 days post infection.

	GF		CV		CVN		LPS	
Functional categories	NI	10d	NI	10d	NI	10d	NI	10d
NS[1]	480 ± 20	365 ± 4	516 ± 55	443 ± 58	460 ± 40	438 ± 45	486 ± 56	359 ± 16
AF[2]	487 ± 12	467 ± 18	557 ± 9	512 ± 11	530 ± 12	487 ± 12	554 ± 18	507 ± 10
MB[3]	733 ± 24	**463** ± 54*	671 ± 23	567 ± 15	710 ± 20	565 ± 49	662 ± 9	551 ± 30
RSF[4]	360 ± 18	**298** ± 31*	380 ± 12	343 ± 17	370 ± 12	350 ± 0	360 + 10	335 ± 15
MT[5]	225 ± 0	**93** ± 27*	220 ± 5	**135** ± 6*	220 ± 5	**125** ± 27*	225 ± 0	**143** ± 15*

GF: Germfree, CV: Conventional, CVN: Conventionalized and LPS: LPS-stimulated mice. NI: Non-infected mice. 10d: Score 10 days after infection. The tasks were grouped into five functional categories: neuropsychiatric state (NS[1]), autonomic function (AF[2]), motor behavior (MB[3]), reflex and sensory function (RSF[4]), muscle tone and strength (MT[5]). The results are presented mean ± SEM of six animals in each group. Scores of the infected groups were compared with the uninfected group by the Wilcoxon matched test.

* $p < 0.05$ was considered to be significant.

stimuli to enlargement of the capsule and yeast cell. Likewise, other studies reported these phenotypic alterations of yeasts isolated from immunocompromised patients (Robertson et al., 2014). It is known that bigger cryptococcal cells have reduced penetration in the central nervous system (Okagaki et al., 2010a,b). In this way, the higher fungal burden in the brain of GF mice was also associated to the smaller cells. Indeed, smaller cells adapt to changes in environmental conditions faster than larger cells (Young, 2006) and *Cryptococcus* displays ovoid morphology during transmigration, suggesting that morphological changes are important for infection (Shi et al., 2010).

Conventionalization and LPS stimulation of GF mice reversed the delayed inflammatory profile of GF mice, leading to increased survival. According to a previous study (Fagundes et al., 2012), GF

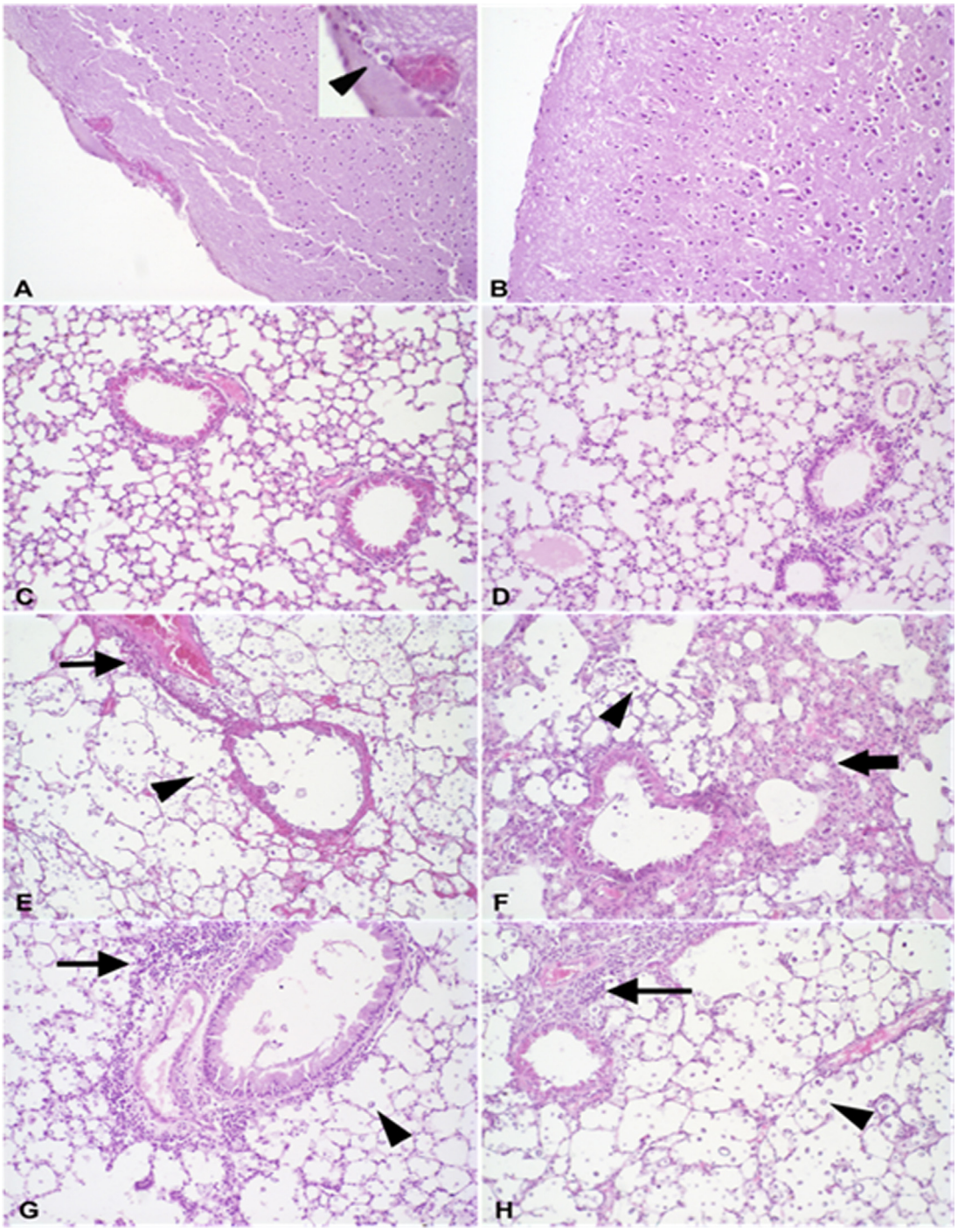

Fig. 6. Delayed inflammation was associated with lower tissue damage in GF mice.
CV, GF, CVN, and LPS mice were inoculated by the intratracheal route with 1×10^7 C. gattii cells or PBS (NI). Brain and lungs were removed for histopathological analysis. (A) GF mice 10 days post inoculation (d.p.i.) showed yeast (arrow head) in the leptomeninge (in detail). (B) No changes were observed in the brain of mice in other groups (CV mice). Lungs of non-inoculated mice: GF(C) and CV (D) groups. Lungs of GF mice at 10 d.p.i. showed numerous yeasts (arrow head), intense hyperemia, and mild perivascular inflammation (arrow) (E). The lungs of CV mice at 10 d.p.i. showed yeasts (arrow head), and moderate interstitial inflammatory infiltrates (large arrow) (F). Lungs of CVN (G) and LPS (H) mice at 10 d.p.i. showed yeast (arrow head), and moderate perivascular and peribronquial inflammation (arrow).H&E, 200×.

mortality may result from an inability to recruit neutrophils to the lungs, which requires MyD-88-dependent signaling by microbiota (Karmarkar and Rock, 2013).

Assessment of *Cryptococcus* interaction with host tissue revealed that this process is strongly influenced by the immune status of the host (Okubo et al., 2013). The intensity of the lesions in the lungs was mild in GF mice and moderate to intense in CV, CVN, and LPS-stimulated mice infected with *C. gattii*. Conversely, GF mice had limited tissue damage due an inefficient immune response. CV, CVN and LPS-stimulated mice exhibited more pronounced tissue damage due to a more substantial immune response.

The SHIRPA battery mimics the human neurological, psychiatric and general parameters of morbidity (Rogers et al., 1997). We used this protocol in this model to evaluate the general health of animals and this parameter confirmed the results showed in the survival curve. Germ-free animals, despite to have the same load fungi in

the brain (10 d.p.i) than other groups, presented more moribund. The behavioral changes were more evident in GF mice, in which *C. gattii* reached the brain at 1 d.p.i., and yeast cells were observed at the meningeal membranes. This early translocation probably led to the more prominent behavioral alterations (Charlier et al., 2008).

In conclusion, this study provides new insights into the important role of microbiota as a stimulus to the immune response during cryptococcosis. Our findings demonstrated that GF mice have delayed immune response against *C. gattii*, therefore the yeasts were smaller and the mice is more susceptible to infection, presenting high fungal burden, more evident alterations in behavior and reduced inflammation.

Conflicts of interest

The authors declare that there are no conflicts of interest.

Acknowledgments

This work was supported by Fundação de Amparo a Pesquisa do Estado de Minas Gerais (Grant PPM-00117-14) and Conselho Nacional de Desenvolvimento Científico e Tecnológico—CNPq (Grant 472438/2013-1). DAS is a research fellow of the CNPq (Grant 305154/2014-1).

Appendix A. Supplementary data

Supplementary data associated with this article can be found, in the online version, at http://dx.doi.org/10.1016/j.ijmm.2016.03.010.

References

Aires, R.D., Capettini, L.S., Silva, J.F., Rodrigues-Machado, M.A.G., Pinho, V., Teixeira, M.M., Cortes, S.F., Lemos, V.S., 2013. Paraquat poisoning induces TNF-α-dependent iNOS/NO mediated hyporesponsiveness of the aorta to vasoconstrictors in rats. PLoS One 8, e73562.

Brouwer, A.E., Siddiqui, A.A., Kester, M.I., Sigaloff, K.C., Rajanuwong, A., Wannapasni, S., Chierakul, W., Harrison, T.S., 2007. Immune dysfunction in HIV-seronegative, *Cryptococcus gattii* meningitis. J. Infect. 54, e165–168.

Charlier, C., Dromer, F., Lévêque, C., Chartier, L., Cordoliani, Y.S., Fontanet, A., Launay, O., Lortholary, O., 2008. Cryptococcal neuroradiological lesions correlate with severity during cryptococcal meningoencephalitis in HIV-positive patients in the HAART era. PLoS One 3, e1950.

Charlier, C., Nielsen, K., Daou, S., Brigitte, M., Chretien, F., Dromer, F., 2009. Evidence of a role for monocytes in dissemination and brain invasion by *Cryptococcus neoformans*. Infect. Immun. 77, 120–127.

Elian, S.D.A., Souza, É.L.S., Vieira, A.T., Teixeira, M.M., Esteves, A.R.M., Nicoli, J.R., Martins, F.S., 2015. Bifidobacterium longum subsp. infantis BB-02 attenuates acute murine experimental model of inflammatory bowel disease. Benef. Microbes 1, 1–10.

Fagundes, C.T., Amaral, F.A., Vieira, A.T., Soares, A.C., Pinho, V., Nicoli, J.R., Vieira, L.Q., Teixeira, M.M., Souza, D.G., 2012. Transient TLR activation restores inflammatory response and ability to control pulmonary bacterial infection in germfree mice. J. Immunol. 188, 1411–1420.

Ferreira, G.F., Baltazar, L.E.M., Santos, J.R., Monteiro, A.S., Fraga, L.A., Resende-Stoianoff, M.A., Santos, D.A., 2013. The role of oxidative and nitrosative bursts caused by azoles and amphotericin B against the fungal pathogen *Cryptococcus gattii*. J. Antimicrob. Chemother. 68, 1801–1811.

Ferreira, G.F., Santos, J.R., Costa, M.C., Holanda, R.A., Denadai, Â., Freitas, G.J., Santos, Á.R., Tavares, P.B., Paixão, T.A., Santos, D.A., 2015. Heteroresistance to itraconazole alters the morphology and increases the virulence of *Cryptococcus gattii*. Antimicrob. Agents Chemother. 59, 4600–4609.

Fox, A.C., McConnell, K.W., Yoseph, B.P., Breed, E., Liang, Z., Clark, A.T., et al., 2012. The endogenous bacteria alter gut epithelial apoptosis and decrease mortality following *Pseudomonas aeruginosa* pneumonia. Shock 38, 508–514.

Franco-Paredes, C., Womack, T., Bohlmeyer, T., Sellers, B., Hays, A., Patel, K., Lizarazo, J., Lockhart, S.R., Siddiqui, W., Marr, K.A., 2015. Management of *Cryptococcus gattii* meningoencephalitis. Lancet Infect. Dis. 15, 348–355.

Ichinohe, T., Pang, I.K., Kumamoto, Y., Peaper, D.R., Ho, J.H., Murray, T.S., Iwasaki, A., 2011. Microbiota regulates immune defense against respiratory tract influenza A virus infection. Proc. Natl. Acad. Sci. U. S. A. 108, 5354–5359.

Inagaki, H., Suzuki, T., Nomoto, K., Yoshikai, Y., 1996. Increased susceptibility to primary infection with *Listeria monocytogenes* in germfree mice may be due to lack of accumulation of L-selectin+ CD44+ T cells in sites of inflammation. Infect. Immun. 64, 3280–3287.

Kamada, N., Seo, S.U., Chen, G.Y., Núñez, G., 2013. Role of the gut microbiota in immunity and inflammatory disease. Nat. Rev. Immunol. 13, 321–335.

Karmarkar, D., Rock, K.L., 2013. Microbiota signalling through MyD88 is necessary for a systemic neutrophilic inflammatory response. Immunology 140, 483–492.

Khosravi, A., Yáñez, A., Price, J.G., Chow, A., Merad, M., Goodridge, H.S., Mazmanian, S.K., 2014. Gut microbiota promote hematopoiesis to control bacterial infection. Cell Host Microbe. 15, 374–381.

Kuss, S.K., Best, G.T., Etheredge, C.A., Pruijssers, A.J., Frierson, J.M., Hooper, L.V., Dermody, T.S., Pfeiffer, J.K., 2011. Intestinal microbiota promote enteric virus replication and systemic pathogenesis. Science 334, 249–252.

Lackner, P., Beer, R., Heussler, V., Goebel, G., Rudzki, D., Helbok, R., Tanniche, E., Schmutzhard, E., 2006. Behavioural and histopathological alterations in mice with cerebral malaria. Neuropathol. Appl. Neurobiol. 32, 177–188.

Lavelle, E.C., Murphy, C., O'Neill, L.A., Creagh, E.M., 2010. The role of TLRs, NLRs, and RLRs in mucosal innate immunity and homeostasis. Mucosal Immunol. 3, 17–28.

Lv, P., Li, H.Y., Ji, S.S., Li, W., Fan, L.J., 2014. Thalidomide alleviates acute pancreatitis-associated lung injury via down-regulation of NFκB induced TNF-α. Pathol. Res. Pract. 210, 558–564.

Ma, H., Hagen, F., Stekel, D.J., Johnston, S.A., Sionov, E., Falk, R., Polacheck, I., Boekhout, T., May, R.C., 2009. The fatal fungal outbreak on Vancouver Island is characterized by enhanced intracellular parasitism driven by mitochondrial regulation. Proc. Natl. Acad. Sci. U. S. A. 106, 12980–12985.

Maxeiner, J.H., Karwot, R., Hausding, M., Sauer, K.A., Scholtes, P., Finotto, S., 2007. A method to enable the investigation of murine bronchial immune cells, their cytokines and mediators. Nat. Protoc. 2, 105–112.

Mittrücker, H.W., Seidel, D., Bland, P.W., Zarzycka, A., Kaufmann, S.H., Visekruna, A., Steinhoff, U., 2014. Lack of microbiota reduces innate responses and enhances adaptive immunity against *Listeria monocytogenes* infection. Eur. J. Immunol. 44, 1710–1715.

Nardi, R.M., Silva, M.E., Vieira, E.C., Bambirra, E.A., Nicoli, J.R., 1989. Intragastric infection of germfree and conventional mice with *Salmonella* typhimurium. Braz. J. Med. Biol. Res. 22, 1389–1392.

Okagaki, L.H., Strain, A.K., Nielsen, J.N., Charlier, C., Baltes, N.J., Chrétien, F., Heitman, J., Dromer, F., Nielsen, K., 2010a. Cryptococcal cell morphology affects host cell interactions and pathogenicity. PLoS Pathog. 6, e1000953.

Okagaki, L.H., Strain, A.K., Nielsen, J.N., Charlier, C., Baltes, N.J., Chrétien, F., Heitman, J., Dromer, F., Nielsen, K., 2010b. Cryptococcal cell morphology affects host cell interactions and pathogenicity. PLoS Pathog. 17, e1000953.

Okubo, Y., Wakayama, M., Ohno, H., Yamamoto, S., Tochigi, N., Tanabe, K., Kaneko, Y., Yamagoe, S., Umeyama, T., Shinozaki, M., Nemoto, T., Nakayama, H., Sasai, D., Ishiwatari, T., Shimodaira, K., Yamamoto, Y., Kamei, K., Miyazaki, Y., Shibuya, K., 2013. Histopathological study of murine pulmonary cryptococcosis induced by *Cryptococcus gattii* and *Cryptococcus neoformans*. Jpn. J. Infect. Dis. 66, 216–221.

Pedroso, V.S.P., Vilela, M.d.C., Santos, P.C., Cisalpino, P.S., Arantes, R.M.E., Rachid, M.A., Teixeira, A.L., 2010. Development of a murine model of neuroparacoccidioidomycosis. J. Neuroparasitol., 39–44.

Pedroso, V.S., Vilela, M.C., Santos, P.C., Cisalpino, P.S., Rachid, M.A., Teixeira, A.L., 2013. Traffic of leukocytes and cytokine up-regulation in the central nervous system in a murine model of neuroparacoccidioidomycosis. Mycopathologia 176, 191–199.

Pedroso, S.H., Vieira, A.T., Bastos, R.W., Oliveira, J.S., Cartelle, C.T., Arantes, R.M., Soares, P.M., Generoso, S.V., Cardoso, V.N., Teixeira, M.M., Nicoli, J.R., Martins, F.S., 2015. Evaluation of mucositis induced by irinotecan after microbial colonization in germ-free mice. Microbiology 161, 1950–1960.

Perfect, J.R., Dismukes, W.E., Dromer, F., Goldman, D.L., Graybill, J.R., Hamill, R.J., Harrison, T.S., Larsen, R.A., Lortholary, O., Nguyen, M.H., Pappas, P.G., Powderly, W.G., Singh, N., Sobel, J.D., Sorrell, T.C., 2010. Clinical practice guidelines for the management of cryptococcal disease: 2010 update by the infectious diseases society of america. Clin. Infect. Dis. 50, 291–322.

Robertson, E.J., Najjuka, G., Rolfes, M.A., Akampurira, A., Jain, N., Anantharanjit, J., et al., 2014. *Cryptococcus neoformans* ex vivo capsule size is associated with intracranial pressure and host immune response in HIV-associated cryptococcal meningitis. J. Infect. Dis. 209, 74–82.

Rogers, D.C., Fisher, E.M., Brown, S.D., Peters, J., Hunter, A.J., Martin, J.E., 1997. Behavioral and functional analysis of mouse phenotype SHIRPA, a proposed protocol for comprehensive phenotype assessment. Mamm. Genome 8, 711–713.

Rogers, D.C., Peters, J., Martin, J.E., Ball, S., Nicholson, S.J., Witherden, A.S., Hafezparast, M., Latcham, J., Robinson, T.L., Quilter, C.A., Fisher, E.M., 2001. SHIRPA, a protocol for behavioral assessment: validation for longitudinal study of neurological dysfunction in mice. Neurosci. Lett. 306, 89–92.

Round, J.L., Mazmanian, S.K., 2009. The gut microbiota shapes intestinal immune responses during health and disease. Nat. Rev. Immunol. 9, 313–323.

Santos, J.R., Holanda, R.A., Frases, S., Bravim, M., Araujo, G.E.S., Santos, P.C., Costa, M.C., Ribeiro, M.J., Ferreira, G.F., Baltazar, L.M., Miranda, A.S., Oliveira, D.B., Santos, C.M., Fontes, A.C., Gouveia, L.F., Resende-Stoianoff, M.A., Abrahão, J.S., Teixeira, A.L., Paixão, T.A., Souza, D.G., Santos, D.A., 2014. Fluconazole alters the polysaccharide capsule of *Cryptococcus gattii* and leads to distinct behaviors in murine Cryptococcosis. PLoS One 9, e112669.

Shi, M., Li, S.S., Zheng, C., Jones, G.J., Kim, K.S., Zhou, H., Kubes, P., Mody, C.H., 2010. Real-time imaging of trapping and urease-dependent transmigration of *Cryptococcus neoformans* in mouse brain. J. Clin. Invest. 120, 1683–1693.

Sommer, F., Bäckhed, F., 2013. The gut microbiota–masters of host development and physiology. Nat. Rev. Microbiol. 11, 227–238.

Souza, D.G., Vieira, A.T., Soares, A.C., Pinho, V., Nicoli, J.R., Vieira, L.Q., Teixeira, M.M., 2004. The essential role of the intestinal microbiota in facilitating acute inflammatory responses. J. Immunol. 173, 4137–4146.

Wilks, J., Beilinson, H., Golovkina, T.V., 2013. Dual role of commensal bacteria in viral infections. Immunol. Rev. 255, 222–229.Yi, P., Li, L., 2012. The germfree murine animal: an important animal model for research on the relationship between gut microbiota and the host. Vet. Microbiol. 157, 1–7.

Young, K.D., 2006. The selective value of bacterial shape. Microbiol. Mol. Biol. Rev. 70, 660–703.

Zaragoza, O., García-Rodas, R., Nosanchuk, J.D., Cuenca-Estrella, M., Rodríguez-Tudela, J.L., Casadevall, A., 2010. Fungal cell gigantism during mammalian infection. PLoS Pathog. 6, e1000945.